Theoretical Investigation of the One-photon and Two-photon Absorption Properties for Star-shaped Polycyclic Aromatic Based on Oligothiophenes-Functionalized Truxenone

Xin Zhou[a], Ai-Min Ren[a], Ji-Kang Feng[a,b*], Xiao-Juan Liu[a]

a State Key Laboratory of Theoretical and Computational Chemistry, Institute of Theoretical Chemistry,

b College of Chemistry, Jilin University, Changchun 130023, China

Abstract

A series of star-shaped π-conjugated organic materials with oligothiophenes as the branches and a functionalized truxenone as the core has been theoretically investigated. The one-photon and two-photon absorption properties of these materials are liable to be tuned by introduction of more thiophene rings. The investigation of the structure-property relationship of these materials has indicated differences between star-shaped oligothiophenes and linear oligothiophenes. The results indicate that the enlargement of the conjugation length of the system is an efficient way to increase the two-photon absorption cross section. In addition, we studied the optical properties of a soluble hyperbranched dendrimer. It is shown that as the increase of conjugation length, an enhancement of the two- photon absorption amplitude is based on that of the parent compound by a factor 7.

Keyword: two-photon absorption, electronic structure, oligothiophenes, truxenone

---

*Corresponding author. E-mail: Jikangf@yahoo.com, FAX number: +86-431-8945942

Introduction

Extensive research efforts have been carried out for the design, synthesis, and characterization of new organic chromophores, oligomers, and polymers with potentially large two-photon absorption cross sections for a variety of photonic applications. These photonic applications include upconverted lasing, [1-3] optical power limiting, [4-6] photodynamic therapy,[7] and three-dimensional microfabrication.[8-10] An understanding of the possible structure-to-property relations for molecular two-photon absorption (TPA) is therefore of great importance, something that already has been acknowledged in studies on organic charge-transfer molecules theoretically and experimentally. [11-14] The effects of varying the electron-donating or electron-accepting strength of end groups, introducing additional groups in the middle to vary the charge redistribution, and varying the effective conjugation length have been proven to be efficient ways in producing structures with enhanced two-photon activity.

Recently, extending the charge-transfer dimension from one to two or even to three dimensions has been attested to be a promising strategy for designing materials with large TPA cross section. Compared with conventional dipolar chromophores with nonlinear optical properties, two-dimensional chromophores with C_3 symmetry (often termed octupolar) have several advantages: they are inherently more transparent, since the lack of a dipole moment often results in negligible solvatochromism; the coupling of excited states can lead to enhanced nonlineartities compared with one-dimensional reference chromophores at practically no cost of transparency; the zero dipole moment should enhance the chance of noncentrosymmetric space groups in crystalline

materials, a necessity for practical applications. [15-17]

There have been some theoretical and experimental reports about the nonlinear optical(NLO) properties of the octupolar molecules, particularly on the TPA response. Cho *et al.* [18] have studied the TPA properties of 1,3,5-tricyano-2,4,6-tris(styryl) benzene derivatives. They showed that the maximum TPA cross section value δ_{max} increases as the donor strength and conjugation length increase. A linear relationship is observed between δ_{max} and the first hyperpolarizability β. Beljonne *et al.* analyzed the role of dimensionality on the TPA response of octupolar compounds. They obtained the conclusion that when taking into account the full chemical structures of representative octupolar molecules, the results of the calculations indicate that an enhancement with much larger than three times associated with an increase in dimensionality and delocalization can be achieved when the core of the chromophore allows significant electronic coupling among the individual arms. [19]

Nevertheless, NLO features of oligomer and polymers, especially scaling of the second hyperpolarizability, γ, with generation number were not systematically studied yet. Cho *et al.* [20] investigated NLO and TPA properties of octupolar oligomers containing 2-12 molecules of 1,3,5-tricyano-2,4,6-*tris*(styryl) benzene derivatives and showed the TPA cross section increases as the number of the octupolar units in the molecules increases and a linear relationship is observed between TPA cross section and the first hyperpolarizability. Most recently, Pei *et al.* [21] synthesized a series of star-shaped polycyclic aromatics with two chromophores: truxenone as the core and oligothiophenes as the branches, which present special intrinsic physical properties of

structural and chemical disorder, and the easy modification of the thiophene structure. In this work, we demonstrate theoretically the electronic structure, one-photon absorption (OPA) and TPA properties of this series of octupolar oligomers.

2. Theoretical Methodology

The TPA process corresponds to simultaneous absorption of two photons. The TPA efficiency of an organic molecule, at optical frequency $\omega/2\pi$, can be characterized by the TPA cross-section $\delta(\omega)$. It can be directly related to the imaginary part of the second hyperpolarizability $\gamma(-\omega;\omega,\omega,-\omega)$ by [22]:

$$\delta(\omega) = \frac{8\pi^2\hbar\omega^2}{n^2c^2} L^4 \,\mathrm{Im}\,\gamma(-\omega;\omega,\omega,-\omega) \qquad (1)$$

where $\hbar$ is Planck's constant divided by 2π, n is the refractive index of medium, c is the speed of light, L is a local field factor (equal to 1 for vacuum).

The sum-over-states (SOS) expression to evaluate the components of the second hyperpolarizability γ_{ijkl} can be induced out using perturbation theory and density matrix method. By considering a power expansion of the energy with respect to the applied field, the methodology adopted here to calculate the second hyperpolarizability are given in the form shown in the literatures [23, 24]. To compare the calculated δ value with the experimental value measured in solution, the orientationally averaged (isotropic) value of γ is evaluated, which is defined as

$$\langle\gamma\rangle = \frac{1}{15}\sum_{i,j}\left(\gamma_{iijj} + \gamma_{ijij} + \gamma_{ijji}\right) \qquad i,j = x,y,z \qquad (2)$$

Whereafter <γ> is taken into the Eq.(1), and then the TPA cross section δ(ω) is obtained.

In principle, any kind of self–consistent field molecular orbital procedure combined with configuration interaction (CI) can be used to calculate the physical values in the above expression. In present paper, the B3LYP/6-31G* method was firstly used to calculate molecular equilibrium geometry. Then, the property of electronic excited state was obtained by 196 single electron excitation and 54 double electron excitation configuration interaction using ZINDO program. Furthermore, UV–vis (ground–state one–photon absorption) spectra which were needed to predict TPA were provided. Then according to the formula (1), (2) and SOS expression, the second hyperpolarizability γ and TPA cross section $\delta(\omega)$ were calculated.

3. Results and discussions

3.1 Geometry optimization and electronic structure

The complexes chosen for the present study are displayed in Figure 1. The molecular geometries are optimized by the B3LYP method [25,26] using the 6-31G* basis set under the constraint symmetry: C_3 for molecules **T1** to **T4**. The dendrimer **M** was synthesized utilizing **T1** by employing the $FeCl_3$ mediated oxidative polymerization in chloroform. Taking into account the size of molecule **M** with C_3 symmetry, the intermolecular geometric parameters were optimized at the semi-empirical Austin Model 1 (AM1) method [27]. The choice of an appropriate one-dimensional reference system for comparison of one-photon and two-photon absorption properties is difficult and to some extent arbitrary since the connecting moiety, truxenone, is strongly coupling and cannot reasonably be divided into subunits. So we use similar one-dimensional reference systems **Sn** (in Figure 1) to compare with octupolar

systems. As for these dipole molecules, there is no constraint of symmetry. The calculations are performed by the G AUSSIAN 03 program package. [28] The optimized structures of **S3**, **T3** and **M** are shown in Figure 2. From the optimized geometries of **Tn** (n=1~4) and **M**, it is seen that the truxenone macrocycle is practically planar. The dihedral angle between the truxenone plane and the thiophene ring is 27.3° (for **T1**), 24.7° (for **T2**), 25.0° (for **T3**) and 25.0° (for **T4**) and the dihedral angle between two thiophene rings is less than 5°. It is obvious that the torsion between the core and thiophene ring contributes to the molecular nonplanarity for **Tn** (n=1~4) and **M**. The nonplanar structures will affect the molecular conjugation and the coupling in each arm of octupolar molecules. As the case of **Sn** (n=1~4), the dihedral angle between the 9,9-dimetylfluorene plane and the thiophene ring is 27.9° (for **S1**), 25.6° (for **S2**), 25.6° (for **S3**) and 25.4° (for **S4**) and the torsional angle between two thiophene rings is averagely 15.6°. The coplanarity of dipolar molecules **Sn** is worse than that of octupolar molecules **Tn**.

It is often possible to ascertain the energy gap (ΔE) between the highest occupied orbital (HOMO) and the lowest unoccupied orbital (LUMO) of polymers (conjugation length tending to infinity) by examination of the plot of ΔE between HOMO and LUMO versus the quantity 1/*N*, where *N* represents the oligomeric length. In this study, we have chosen *N* to equal to the number of thiophene rings in **Sn** (n=1~4) and in each arm of **Tn** (n=1~4). As shown in Figure 3(a) and 3(b), the plots using the data points obtained for the oligomers by using B3LYP/6-31G* method are reasonably linear. The inset in Figure 3(b) shows the experimental result of octupolar

oligothiophenes measured in THF solution in the supporting information of literature 21. The linear equations showed a saturation limit for ΔE vs the number of thiophene rings:

L1: $\Delta E = 1.43/n + 2.56$ (for octupolar molecules)

L2: $\Delta E = 0.94/n + 2.71$ (experimental result for octupolar molecules)

L3: $\Delta E = 1.59/n + 2.61$ (for dipolar molecules)

The result above shows that the calculated slope of the line (L1) constructed by octupolar molecules is larger than the experimental value (L2) and the intercept of L1 is slightly smaller than that of L2. The reason of dissimilarities between two intercepts and slopes for octupolar oligothiophenes is that experimentally the lowest energy transition is used to depict the plot, which is almost equal to the energy gap between HOMO and LUMO. This equality depends on two preconditions: firstly the lowest excited singlet state is constructed by the transition from HOMO to LUMO, and secondly all solvent effects are neglected. As shown in the transition nature in Table 1, the transition from HOMO to LUMO plays a minor role in the lowest excited states for octupolar oligothiophenes; however, the deeper energy transitions are the main contribution to the lowest excited states of them. Observing two slopes of L1 and L3, one can find that the slope of L3 is larger than that L1, which indicates dipolar oligothiophenes reach a saturation limit for ΔE vs the number of thiophene moieties more easily than octupolar ones. The obtained linear equations can be used to calculate the energy gap between HOMO and LUMO for analogical polythiophenes.

3.2 One-photon Absorption

On the basis of optimized molecular structures by B3LYP/6-31G* method, we calculated the OPA spectra (UV-vis spectra) for all chromphores using the ZINDO program. Table 1 shows the maximum OPA wavelength $\lambda^{(1)}_{max}$, the corresponding oscillator strength *f* and transition nature for every compound. As shown in Table 1, the electronic absorption behavior of these star-shaped oligothiophenes exhibited a perfect correlation to the conjugation length, i.e., the one-photon absorption maximum was continuously red-shifted as the effective conjugated length of the respective oligothiophene branches increased. **T1**, **T2**, **T3** and **T4** exhibited maximum absorptions at 331.2, 372.6, 407.0 and 435.3 nm, respectively, and were substantially red-shifted relative to the linear compounds **Sn** (296.4 nm for **S1**, 351.4 nm for **S2**, 387.0 nm for **S3** and 427.2 nm for **S4**). Such a red-shift is due to the π-electron delocalization through the truxenone core among the branches together with the contributions from the additional central truxenone segment. Although the calculated values, $\lambda^{(1)}_{max}$ are quantitatively a bit different from the experimental data, the general trend of increasing $\lambda^{(1)}_{max}$ with respect to the conjugated length is in an excellent agreement with the experiment. These differences are most likely due to a combination of gas phase modeling and replacement of dihexyl by computationally simpler dimethyl groups.

As can be seen in Table 1, the molecular length determines importantly the OPA intensities of oligothiophenes. The oscillator strength of dipolar oligothiophenes **Sn** (n=1~4) increases continuously as the increase in the conjugation length and varies over the range from 0.96688 (for **S1**) to 1.35148 (for **S2**) to 1.64351 (for **S3**) and to

1.95707 (for **S4**). As the case of octupolar oligothiophenes **Tn**(n=1~4), the same trend is detected. As shown in Table 1, molecules **Tn** (n=1~4) have two degenerate excited states, possessing the same intensity since the symmetry of them is C_3. The oscillator strength of **T1** is found to be 3.6881, which is larger than that of **S1** by a factor of 3.8. The intensity of OPA increases by a same factor of 3.2, when going from **S2** to **T2**, from **S3** to **T3**, and from **S4** to **T4**. This implies that the oscillator strength of octupolar oligothiophenes **Tn** (n=1~4) is the sum of that of each branch.

The OPA properties of the soluble hyperbranched dendrimer **M** optimized by AM1 method are also listed in Table 1. The calculated result shows that there are two OPA maximums with the almost same intensity at 406.5 nm and 310.1 nm, which are basically line with the experimental result [21]. The first OPA maximum at 406.5 nm is red-shifted about 74 nm in comparison with that of the parent **T1,** which is close to the experimental value of 64 nm [21]. Though the results obtained by AM1 and B3LYP methods cannot directly be compared, the trend of parameters can be considered qualitatively.

3.3 Two-photon absorption

Generally, the position and relative strength of the two-photon resonance are to be predicted using the following simplified form of the SOS expression [11,29]:

$$\delta \propto \frac{M_{0k}^2 M_{kn}^2}{\left(E_{0k} - E_{0n}/2\right)^2 \Gamma} \qquad (3)$$

where M_{ij} is the transition dipole moment from the state i to j; E_{ij} is the corresponding excitation energy, the subscripts 0, k and n refer to the ground state S_0, the virtual intermediate state S_k and the TPA final state S_n respectively□Γ is the

damping factor. We consider that the higher the excited state, the shorter its lifetime, and express the damping, in eV, as [30]

$$\Gamma_{mo} = 0.08 \times \frac{\omega_{mo}}{\omega_{1o}} \qquad (4)$$

According to expressions (1), (2) and SOS equation [23,24], we compiled a program to calculate the second hyperpolarizability γ and the TPA cross section $\delta(\omega)$. In this paper, on the basis of Eq. (3)-the three-state approximation, we select the excited states with the biggest M_{0k} and M_{kn} (shown in Figure 4), and regard the n state as the final state of TPA, equal to the position of the maximum TPA ($\lambda_{max}^{(2)}$). The TPA cross section at this wavelength is the maximum TPA cross section (δ_{max}). $\lambda^{(2)}_{max}$, δ_{max} and the second hyperpolarizability are summarized in Table 2.

Up to now, there is no report on the NLO or TPA properties of this series of oligothiophenes experimentally, so here we predict theoretically the trend of the TPA properties for oligothiophenes with increasing molecular length rather than the absolute values. As shown in Table 2, with the increased π-electron delocalization and effective conjugation length of the whole molecule after the attachment of more thiophene segments, the basically continuous red shifts of the TPA peak for molecules are observed (from 526.8 nm for **S1** to 663 nm for **S4** and from 520 nm for **T1** to 649.4 nm for **T4**).

Inspecting the calculated TPA cross sections of the dipolar molecules **Sn** (n=1~4), listed in Table 2, one finds that the TPA cross section value increases by a factor of 1.7, 2.5, 3.4 when going from **S1** to **S2**, to **S3** and to **S4** respectively. If the enhancement of the TPA cross-section with the number of thiophene rings can be expressed

as $\delta_{TPA}(N) = N^{\alpha}\delta_{TPA}(N=1)$, α value varies over the range from 0.8 to 0.9.

In the case of **Tn** (n=1~4), the TPA cross section values are in the range of (1469~4660)×$10^{-50}$$cm^4$s/photon and increase monotonically with the increasing number of the thiophene ring within the molecule. The evolution of the TPA magnitude with the number of thiophene moieties in each arm of octupolar molecules can be written as $\delta_{TPA}(N) = N^{\alpha}\delta_{TPA}(N=1)$, α=0.4 ~0.9. In order to obtain α value, we depicted the plot of $\lg\delta_{TPA}(N)$ versus lg*N* according to $\lg\delta_{TPA}(N) = \alpha\lg N + \lg\delta_{TPA}(N=1)$ (shown in Figure 5) and the linear equations are shown as follows:

$$\lg\delta_{TPA}(N) = 0.88\lg N + 2.62 \text{ (for dipolar oligofluorenes)}$$

$$\lg\delta_{TPA}(N) = 0.72\lg N + 3.09 \text{ (for octupolar oligofluorenes)}$$

The equations show that α value for dipolar oligluorenes and octupolar ones is 0.88 and 0.72 respectively.

From the results above, we can find $\alpha_{dipolar} > \alpha_{octupolar}$. In other words, the rate of the increase in the TPA cross section with the number of thiophene for dipolar oligothiophenes is faster than that for octupolar ones. This is due to the fact that the size of octuopolar oligothiophenes **Tn** is relatively larger than that of dipolar analogs, and so the addition of thiophene rings play a comparatively lesser role in the increase of TPA cross section.

In order to further explain the TPA enhancement with the increase of chain length, we apply the exciton model [31] to calculate the evolution of the electronic state parameters when changing the oligomer length (*N*). In this model, assuming that the

transition dipole moments have only one component directed along the long-axis of the molecule, the evolution of the transition dipole moment with the oligomer length *N* can be expressed as:

$$M_{0k}(N) = N^{1/2} M_{0k}(N=1) \qquad (5)$$

$$M_{kn}(N) = N^{1/2} M_{kn}(N=1) \qquad (5')$$

Combining Eqs. (3), (5) and (5') and neglecting the influence of the denominator in Eq. (3), the increase of the TPA cross section with the oligomer length can be written as:

$$\delta_{TPA}(N) = N^2 \delta_{TPA}(N=1) \qquad (6)$$

The behavior $\delta_{TPA}(N) = N^2 \delta_{TPA}(N=1)$ was observed in molecular aggregates and dendrimers with dipole-dipole coupling (Frenkel excitons) [32,33]. However, in this paper, similar scaling behavior is not found. The calculated value of α is smaller than 2. The reason of this result is as follow.

Examining the results shown in Figure 4, we can rationalize the increase in the TPA cross section on going from **S1** to **S4** and **T1** to **T4** on the basis of an increase in the S_0 to S_k transition dipole moment (M_{0k}) from 7.8D (for **S1**) to 13.3D (for **S4**) and from 11.4D (for **T1**) to 17.2D (for **T4**) and a decrease in the detuning term from 3.01eV (for **S1**) to 1.97eV (for **S4**) and from 2.55eV (for **T1**) to 1.90eV (for **T4**). However, the decrease in the S_k to S_n transition dipole moment (M_{kn}) from 6.9D (for **S1**) to 4.1D (for **S4**) and from 6.7D (for **T1**) to 5.5D (for **T4**) gives the negative contribution to the increase of TPA cross section. On the other hand, the power law $\delta_{TPA}(N) = N^2 \delta_{TPA}(N=1)$ was obtained by investigate the linear oligomers including several same monomers. Whereas, in present work, the repeated unit is a segment in

the monomer rather than the whole monomer. Taken together these factors are consistent with the increase of TPA cross section without complying with the law $\delta_{TPA}(N) = N^2\delta_{TPA}(N=1)$.

Now, we compare the TPA cross section of octupolar oligothiophenes with that of dipolar counterparts. The ratios of TPA cross section between two series are as follows: δ_{T1}/δ_{S1}=3.1, δ_{T2}/δ_{S2}=2.4, δ_{T3}/δ_{S3}=2.0, δ_{T4}/δ_{S4}=3.0. Observing the results, we can find an increase by a factor of equal to or less than 3 in the TPA cross section of the octupolar molecule with respect to the isolated arm occurs. The reason for these results is that the functionalized truxene core maintains large distance between the conjugated branches, thus preventing strong through-space electronic interactions between arms as well as sterical hindrances which could hamper intramolecular charge redistribution. The torsion between the core and thiophene rings affects the molecular conjugation and the coupling in each arm of octupolar molecules. Similar results were observed by Brédas and coworkers in reference 19.

As shown in Table 2, comparing the TPA properties of **T1** and **M**, we notice a red shift of the TPA resonance from 520 to 561.2 nm due to an increase of the conjugation length, and an enhancement of the TPA amplitude by a factor 7. It is obvious that the hyperbranched dendrimer is a promising TPA material and worth further being investigated experimentally.

4. Conclusion

A systematically theoretical study on the electronic structure, OPA and TPA properties of octupolar oligothiophenes with dipolar analogs has been performed. The

calculated results show that an increase of in the transition dipole moment (M_{0k}) between the ground state and the lowest excited state and a decrease in the detuning term (E_{0k}-E_{0n}/2) contribute importantly to the increase of TPA cross section. For this series of oligothiophenes, a power law $\delta_{TPA}(N) = N^{\alpha}\delta_{TPA}(N=1)$, α=0.88, 0.72 (for dipolar and octupolar molecules respectively) has been obtained. This abnormal result is owing to the fact that the decrease in the S_k to S_n transition dipole moment (M_{kn}) play a negatively role in the increase of TPA cross section and the power law above-mentioned is not absolutely applicable to this series of oligothiophenes. Deviations from the factor 3 increase in the TPA cross section of octupolar molecules with respect to that of the corresponding dipolar ones can be accounted for the fact that functionalized truxenone core maintains large distance between the conjugated branches, thus preventing strong through-space electronic interactions between arms as well as sterical hindrances which could hamper intramolecular charge redistribution.

Acknowledgements

This work is supported by the National Nature Science Foundation of China (20273023, 90101026) and the Key Laboratory for Supramolecular Structure and Material of Ministry of Education in Jilin University.

Reference

1 J.D. Bhawalkar, G.-S. He, P.N.Prasad , *Prog. Phys.,* 1996, **59**, 1041.

2 G.-S.He, C.-F. Zhao, J.D.Bhawalkar, P.N.Prasad, *Appl.Phys.Lett.,* 1995, **67**, 3703.

3 C.-F. Zhao, G.-S.He, J.D.Bhawalkar, C.K.Park,C.K.; P.N.Prasad, *Chem.Mater.,* 1995, **7**, 1979.

4 P.A.Fleitz, R.A.Sutherland, F.P.Stroghendl, F.P.Larson, L.R.Dalton, *SPIE Proc.,* 1998, **3472**, 91.

5 G.-S.He, J.D.Bhawalkar, C.-F. Zhao, P.N.Prasad, *Appl.Phys.Lett.,* 1995, **67**, 2433.

6 J.E.Ehrlich, X.-L.Wu, I.-Y.S.Lee, Z.-Y. Hu, H.Röeckel, S.R.Marder, J.W.Perry, *Opt.Lett.,* 1997, **22**, 1843.

7 J.D.Bhawalkar, N.D. Kumar, C.-F. Zhao, P.N.Prasad, *J.Clin.Laser Med. Surg*., 1997, **15**, 201.

8 M.Denk , J.H.Strickler , W.W.Webb, *Science,* 1990, **248**, 73 .

9 C.M.J.Xu , W.W.Webb, *Opt . Lett.,* 1995, **20**, 2532 .

10 E. S. Wu, J.H.Stricker, W. R.Harrell, W.W.Webb, *SPIE Proc.,* 1992, **1674**, 776.

11 M.Albota, D.Beljonne, J.L.Brédas, J.E.Ehrlich, J.Fu, A.A.Heikal, E.Hess, T.Kogej, M.D.Levin, S.R.Marder, D.McCord-Maughon, W.Perry, H.Röeckel, M.Rumi,G. Subramaniam, W.W.Webb, X.Wu, C.Xu, *Science,* 1998, **281**, 1653.

12 M.Rumi, J.E.Ehrlich, A.A.Heikal, J.W.Perry, S.Barlow, Z.Hu, D.McCord-Maughon, T.C.Parker, H. Röeckel, S.Thayumanavan, S.R.Marder, D.Beljonne, J.L.Brédas, *J.Am.Chem.Soc.,* 2000, **122**, 9500.

13 P.Norman, Y.Luo, H.Ågren, *J.Chem.Phys.,* 1999, **111**, 7758.

14 C.K.Wang, P.Macak, Y.Luo, H.Ågren, *J.Chem.Phys.,* 2001, **114,** 9813.

15 J.Zyss, I.Ledoux, *Chem.Rev.,* 1994, **94**, 77.

16 J.J.Wolff, R.Wortmann, *J.Prakt.Chem.,* 1998, **340**, 99.

17 M.S.Wong, C.Bosshard, P.Günter, Adv.Mater., 1997, **9**, 837.

18 B.R.Cho, K.H.Son, S.H.Lee, Y.-S.Song, Y.-K.Lee, S.-J.Jeon, J.H.Choi, H.Lee, H.Lee, M.Cho, *J.Am.Chem.Soc.,* 2001, **123**, 10039.

19 D.Beljonne, W.Wenseleers, E.Zojer, Z.-G.Shuai, H.Vogel, S.J.K.Pond, J.W.Perry, S.R.Marder, J.-L.Brédas, *Adv.Funct.Mater.*, 2002, **12**, 631.

20 B.R.Cho, M.J.Piao, K.H.Son, S.H.Lee, S.J.Yoon, S.-J.Jeon, M.Cho, *Chem.Eur.J.,* 2002, **8**, 3907.

21 J.Pei, J.-L.Wang, X.-Y.Cao, X.-H.Zhou, W.-B.Zhang, *J.Am.Chem.Soc.,* 2003, **125**, 9944.

22 C.L.Caylor, I.Dobrianow, C. Kimmr, R.E. Thome, W. Zipfel, W.W. Webb, *Phys. Rev. E.,* 1999, **59 (4)**, R3831.

23 B.J. Orr, J.F.Ward, *Mol.Phys.*, 1971, **20**, 513.

24 D. Beljonne, J. Cornil, Z. Shuai, J.L. Bredas, F. Rohlfing, D.D.C. Bradlley, W.E. Torruellas, V. Ricci, G.I. Stegeman, *Phys.Rev.B,* 1997, **55**, 1505.

25 A.D.Becke, *J.Chem.Phys.,* 1993, **98**, 5648.

26 C.Lee, W.Yang, R.G.Parr, *Phys.Rev.,* 1998, **37**, 786.

27 M.J.S.Dewar, E.G.Zoebisch, E.F.Healy, J.J.P.Stewart, *J.Am.Chem.Soc.*, 1995, **107**, 3702.

28 Æ.Frisch, M.J.Frisch et al., GAUSSIAN 03, Revision A.1, Gaussian Inc., Pittsburgh, PA, 2003.

29 B.Dick, R.M. Hochstrasser, H.P. Trommsdorff, in *Nonlinear Optical Properties of Organic Molecules and Crystals*, Chemla,D.S.; J.Zyss,Eds. (Academic Press, Orlando, FL, 1987), *vol.2*, pp. 167-170.

30 Z.Shuai, J.L.Brédas, *Phys.Rev.B*, 1991, **44**, 5962.

31 E.G.McRae, M.Kasha, *J.Chem.Phys.*, 1958, **28**, 721.

32 Y.Nomura, T.Shibuya, *J.Phys.Soc.Jpn.*, 2002, **71**, 767.

33 F.C.Spano, S.Mukamel, *Phys.Rev.Lett.*, 1991, **66**, 1197.

Table 1 Maximum one-photon absorption and nature of the transition for each compound

Compound	$\lambda_{max}^{(1)}$/*nm*	f	*Transition nature (configurations and weights)*
S1	296.4	0.96688	$S_0 \rightarrow S_1$ (HOMO,0)→(LUMO,0) 86%
S2	351.4	1.35148	$S_0 \rightarrow S_2$ (HOMO,0)→(LUMO,0) 94%
S3	387.0	1.64351	$S_0 \rightarrow S_2$ (HOMO,0)→(LUMO,0) 93%

S4	427.2	1.95707	$S_0 \rightarrow S_2$ (HOMO,0)→(LUMO,0) 92%
T1	331.2	1.84405	$S_0 \rightarrow S_2$ (HOMO,0)→(LUMO+2,0) 25%
	(341) [21]		(HOMO,0)→(LUMO,0) 20%
			(HOMO-1,0)→(LUMO+1,0) 20%
			(HOMO-2,0)→(LUMO,0) 19%
	331.2	1.84405	$S_0 \rightarrow S_3$ (HOMO-1,0)→(LUMO+2,0) 25%
			(HOMO,0)→(LUMO+1,0) 20%
			(HOMO-1,0)→(LUMO,0) 20%
			(HOMO-2,0)→(LUMO+1,0) 19%
T2	372.6	2.13664	$S_0 \rightarrow S_1$ (HOMO,0)→(LUMO+2,0) 29%
	(383)[21]		(HOMO-2,0)→(LUMO,0) 28%
			(HOMO,0)→(LUMO,0) 15%
			(HOMO-1,0)→(LUMO+1,0) 15%
	372.6	2.13664	$S_0 \rightarrow S_2$ (HOMO-1,0)→(LUMO+2,0) 29%
			(HOMO-2,0)→(LUMO+1,0) 28%
			(HOMO,0)→(LUMO+1,0) 15%
			(HOMO-1,0)→(LUMO,0) 15%
T3	407.0	2.65957	$S_0 \rightarrow S_1$ (HOMO,0)→(LUMO+2,0) 30%
	(411)[21]		(HOMO-2,0)→(LUMO,0) 30%
			(HOMO,0)→(LUMO+1,0) 15%
			(HOMO-1,0)→(LUMO,0) 15%
	407.0	2.65957	$S_0 \rightarrow S_2$ (HOMO-1,0)→(LUMO+2,0) 30%
			(HOMO-2,0)→(LUMO+1,0) 29%
			(HOMO,0)→(LUMO,0) 14%
			(HOMO-1,0)→(LUMO+1,0) 14%
T4	435.3	3.18927	$S_0 \rightarrow S_1$ (HOMO,0)→(LUMO+2,0) 30%
	(424)[21]		(HOMO-2,0)→(LUMO,0) 29%
			(HOMO,0)→(LUMO,0) 13%
			(HOMO-1,0)→(LUMO+1,0) 13%
	435.3	3.18927	$S_0 \rightarrow S_2$ (HOMO-1,0)→(LUMO+2,0) 30%
			(HOMO-2,0)→(LUMO+1,0) 29%
			(HOMO,0)→(LUMO,0) 13%
			(HOMO-1,0)→(LUMO+1,0) 13%
M	406.5	2.82457	$S_0 \rightarrow S_1$ (HOMO,0)→(LUMO+2,0) 29%
	(405) [21]		(HOMO-2,0)→(LUMO,0) 28%
			(HOMO,0)→(LUMO,0) 16%
			(HOMO-1,0)→(LUMO+1,0) 16%
	406.5	2.82457	$S_0 \rightarrow S_2$ (HOMO-1,0)→(LUMO+2,0) 29%
			(HOMO-2,0)→(LUMO+1,0) 28%
			(HOMO,0)→(LUMO+1,0) 16%
			(HOMO-1,0)→(LUMO,0) 16%
	310.1	2.84039	$S_0 \rightarrow S_5$ (HOMO-6,0)→(LUMO+4,0) 11%
	(352)[21]		(HOMO-5,0)→(LUMO+6,0) 14%
	310.1	2.84030	$S_0 \rightarrow S_6$ (HOMO-4,0)→(LUMO+7,0) 18%

	(HOMO-4,0)→(LUMO+8,0) 11%
	(HOMO-7,0)→(LUMO+5,0) 11%

Table 2 the two-photon absorption properties of molecules

Compound	$\lambda_{max}^{(2)}$/nm	*Transition*	$\gamma \times 10^{-34}$/esu	$\delta_{max}/10^{-50}$ cm^4s/photon
S1	526.8	$S_0 \rightarrow S_4$	0.02+6.25i	465
S2	623.0	$S_0 \rightarrow S_2$	2.68+15.3i	813
S3	606.6	$S_0 \rightarrow S_3$	22.9+20.4i	1147
S4	663.0	$S_0 \rightarrow S_3$	43.8+33.5i	1573
T1	520.0	$S_0 \rightarrow S_7$	5.48+19.2i	1469
T2	580.0	$S_0 \rightarrow S_7$	-27.1+32.4i	1993
T3	622.2	$S_0 \rightarrow S_6$	-64.1+42.9i	2287
T4	649.4	$S_0 \rightarrow S_6$	-113+95.2i	4660
M	561.2	$S_0 \rightarrow S_{14}$	-311+156i	10260

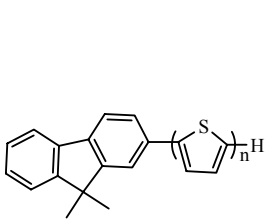

S_1-S_4: n=1- 4

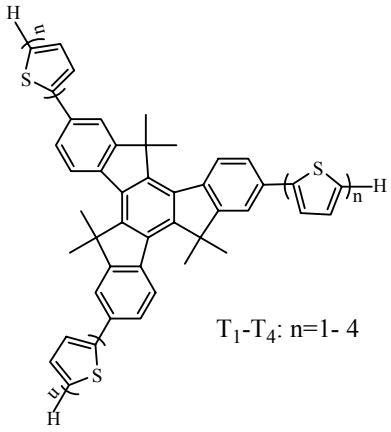

T_1-T_4: n=1- 4

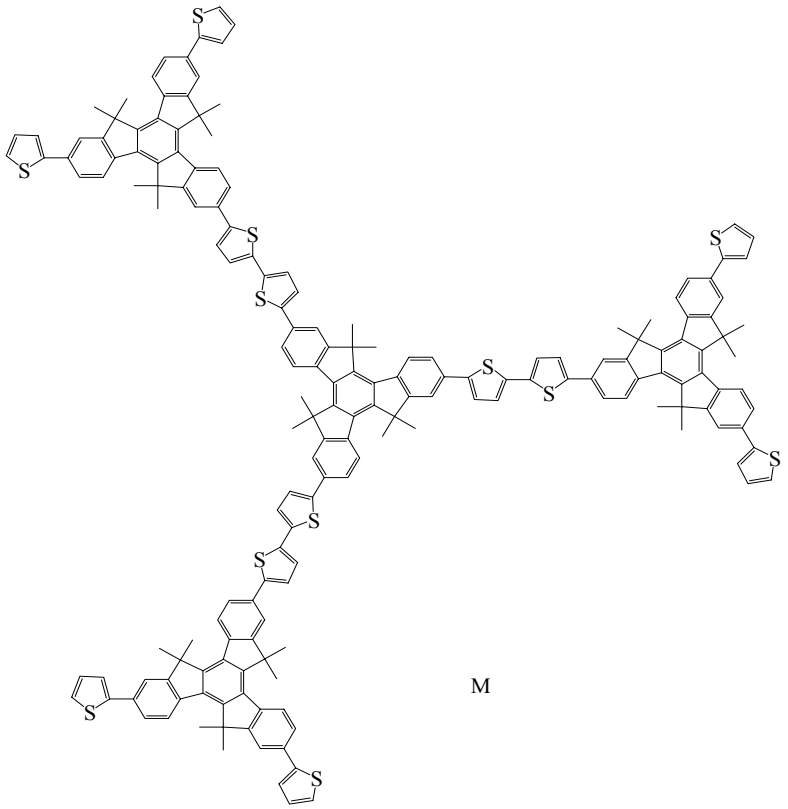

M

Figure 1 Chemical structure of molecules under study

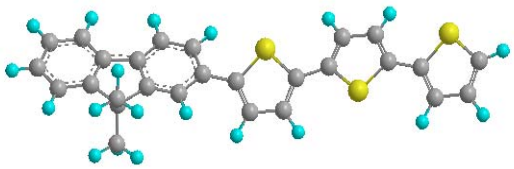

S3

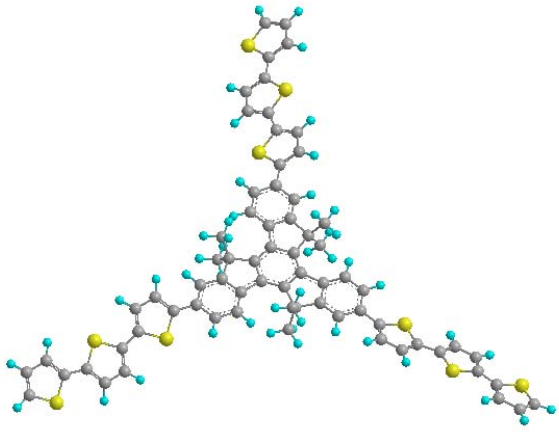

T3

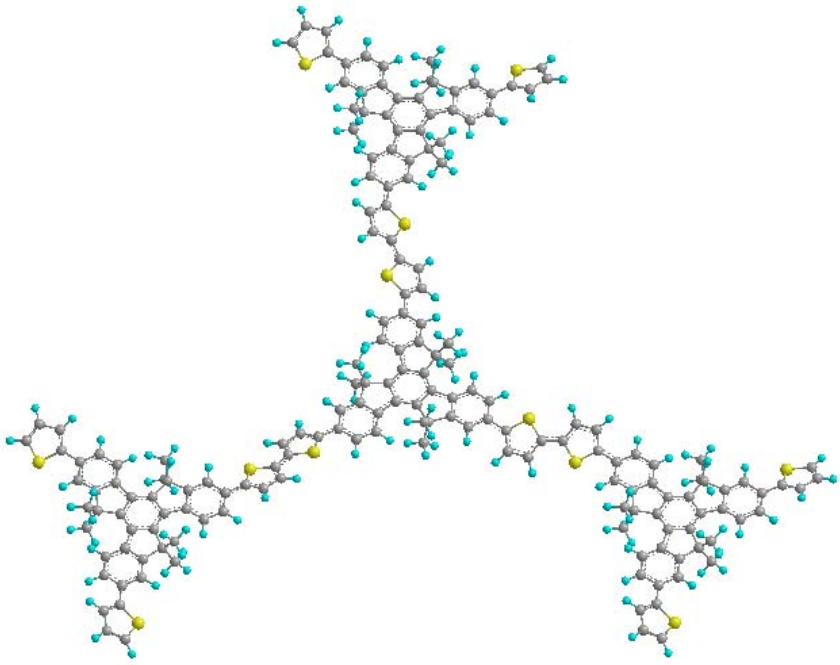

M

Figure 2 Optimized geometries of molecules S3, T3 and M

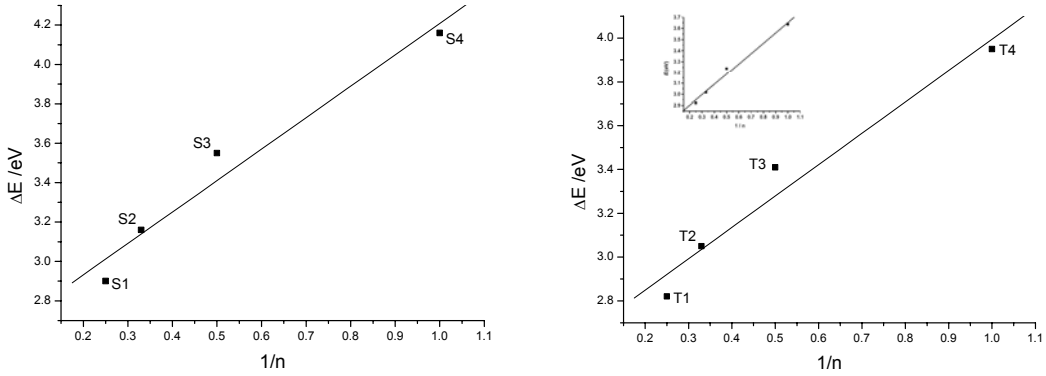

(a) (b)

Figure 3 Energy gap (ΔE) between HOMO and LUMO for compounds vs the inverse ring numbers of thiophenes in the conjugated chromophores (a) for dipolar oligomers (b) for octupolar oligomers

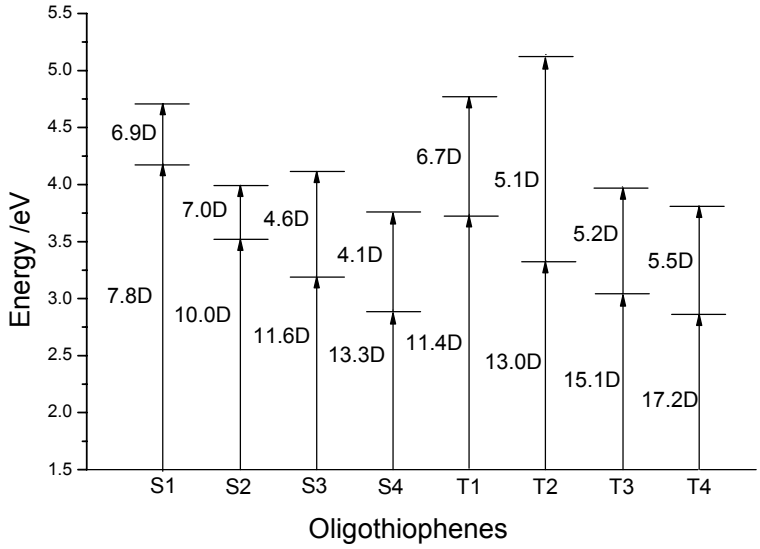

Figure 4 Scheme of the calculated energy levels

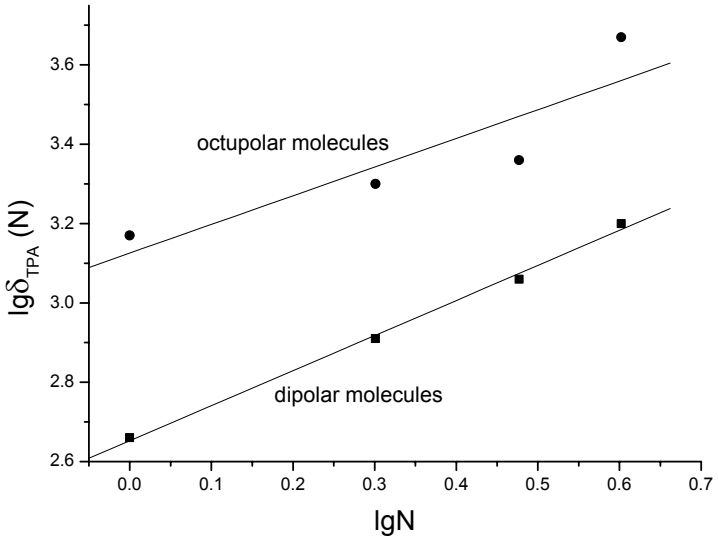

Figure 5 the plot of lg*N* versus lgδ_{TPA}(*N*)